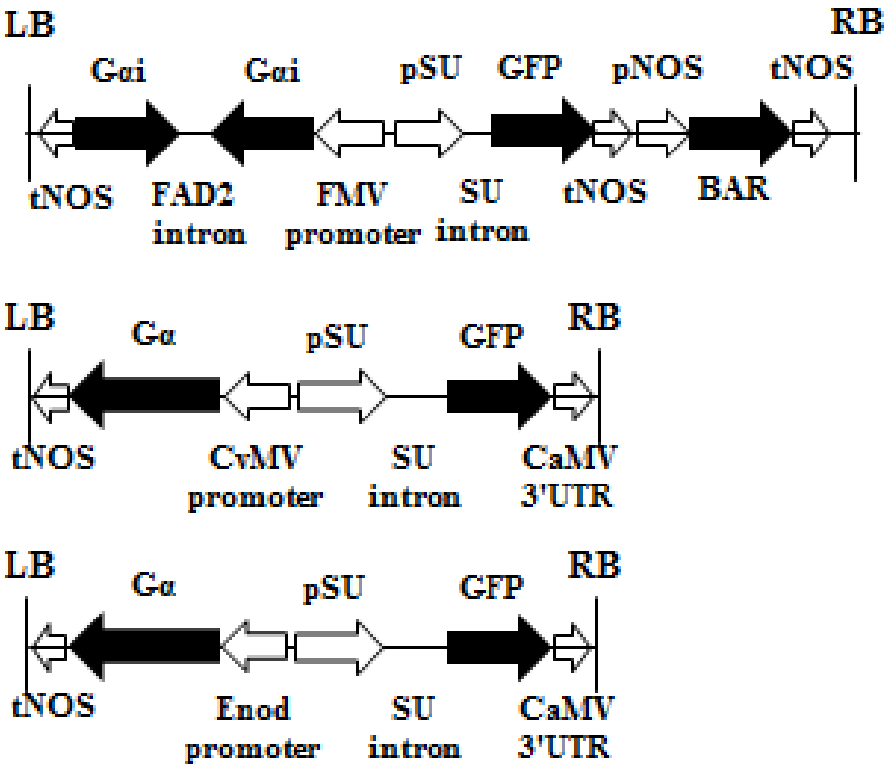

Supplemental Figure 1. Constructs used for RNAi-mediated silencing of soybean *Gα* and *RGS* driven by *FMV* promoter and for overexpression of *Gα* and *RGS* driven by constitutive (*CvMV*) and nodule-specific (*Enod40*) promoter. The selection markers *GFP* and *Bar* are driven by *pSU* promoter and *Nos* promoter, respectively.

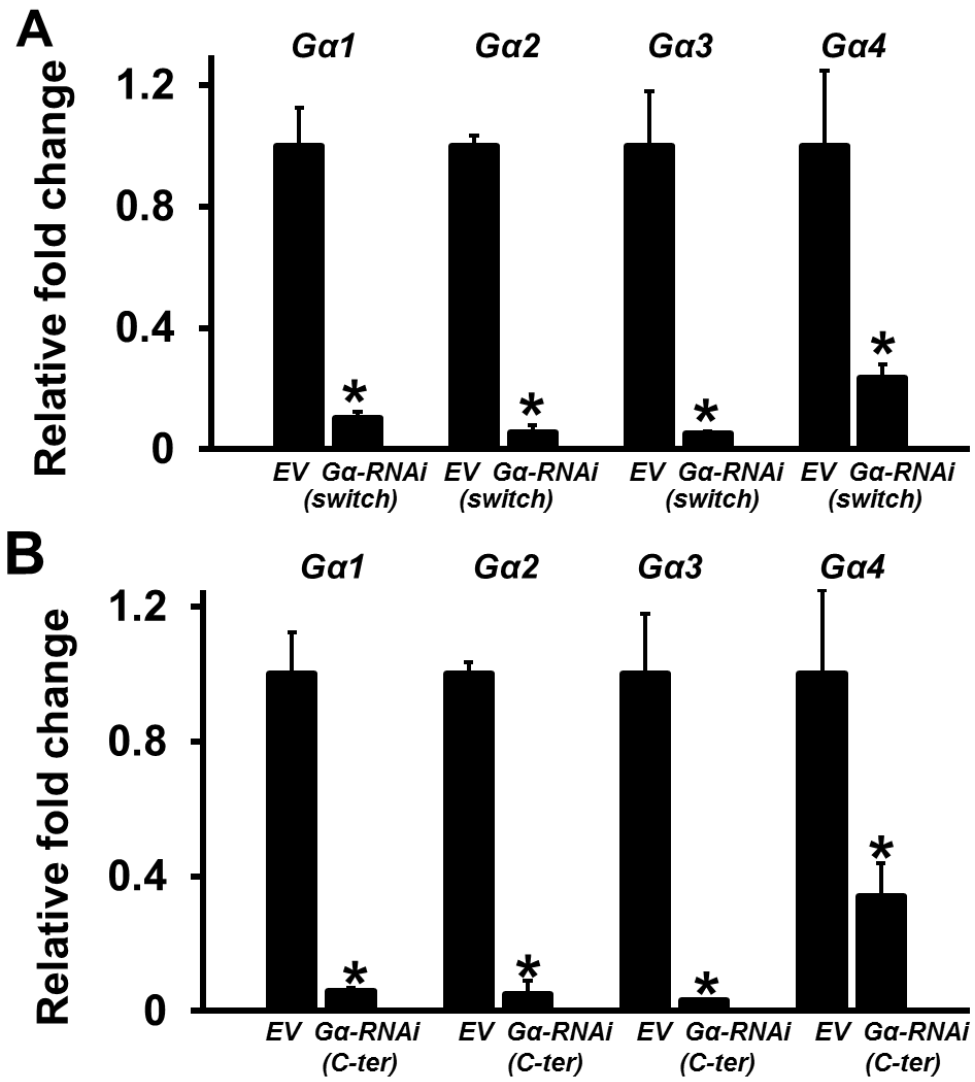

Supplemental Figure 2. Transcript levels of soybean *Gα* genes in *Gα-RNAi* hairy roots and nodulation phenotypes. Hairy roots of soybean were collected from specific *Gα-RNAi* lines at 32 dpi with *B. japonicum*. Expression of individual *Gα* in two different *Gα-RNAi* silenced hairy roots (A) *Gα-RNAi* targeted to the switch region and (B) *Gα-RNAi* targeted to the C-terminal region was measured by real-time quantitative PCR. Fold change represents expression of specific genes in transgenic hairy roots in comparison to empty vector (EV) containing roots, which was set as 1. Data are representative of three independent experiments and are normalized by the reference gene *Actin*. Data are average of two biological replicates each with three different experiments. Error bars represent ± SE. Asterisks (*) indicate statistically significant differences compared to empty vector control (* = $P < 0.05$; Student's *t* test).

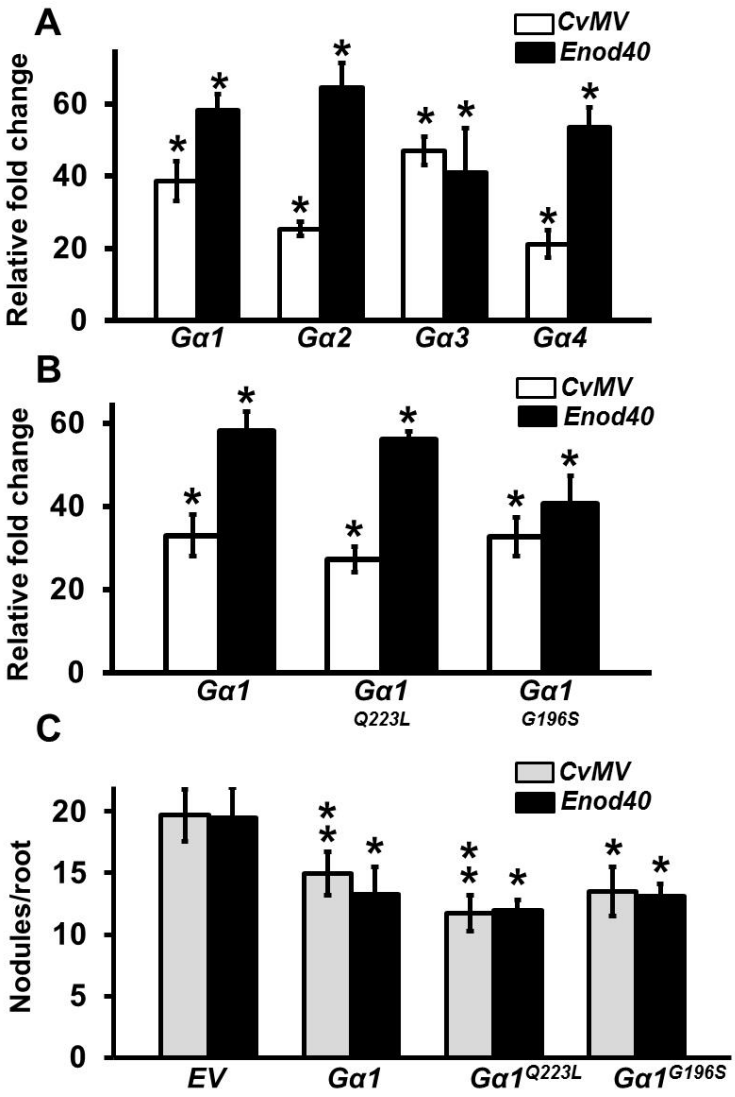

Supplemental Figure 3. Transcript levels of soybean *Gα* genes in *Gα*-overexpressing hairy roots and nodulation phenotypes. Hairy roots of soybean were collected from specific *Gα* over-expression lines at 32 dpi with *B. japonicum*. (A) Expression level of *Gα* genes (1-4) driven by *CvMV* and *Enod40* promoters. (B) Expression level of native and mutant versions of *Gα1* driven by *CvMV* and *Enod40* promoter. Fold change was determined by comparing the transcript levels of specific genes in overexpression lines to their expression in EV control lines. Data are representative of three independent experiments and are normalized by the reference gene *Actin*. Error bars represent ± SE. Asterisks (*) in both A and B indicate statistically significant differences compared to empty vector control (* = $P < 0.05$; Student's *t* test). (C) Nodulation phenotype of transgenic soybean hairy roots expressing native Gα1, constitutively active form of *Gα1* (*Gα1*^{Q223L}) and RGS uncoupler form of *Gα1* (*Gα1*^{G196S}) driven by *CvMV* or *Enod40* promoters. Nodule numbers on transgenic hairy roots was counted at 32 dpi with *B. japonicum* and were compared with their respective empty vector (EV) transformed hairy roots. The data represent average of 3 biological replicates (>40 individual plants/biological replicate containing transgenic nodulated roots). Asterisks (*) indicate statistically significant differences compared to empty vector control (* = $P < 0.05$; ** = $P < 0.01$; Mann-Whitney *U* test).

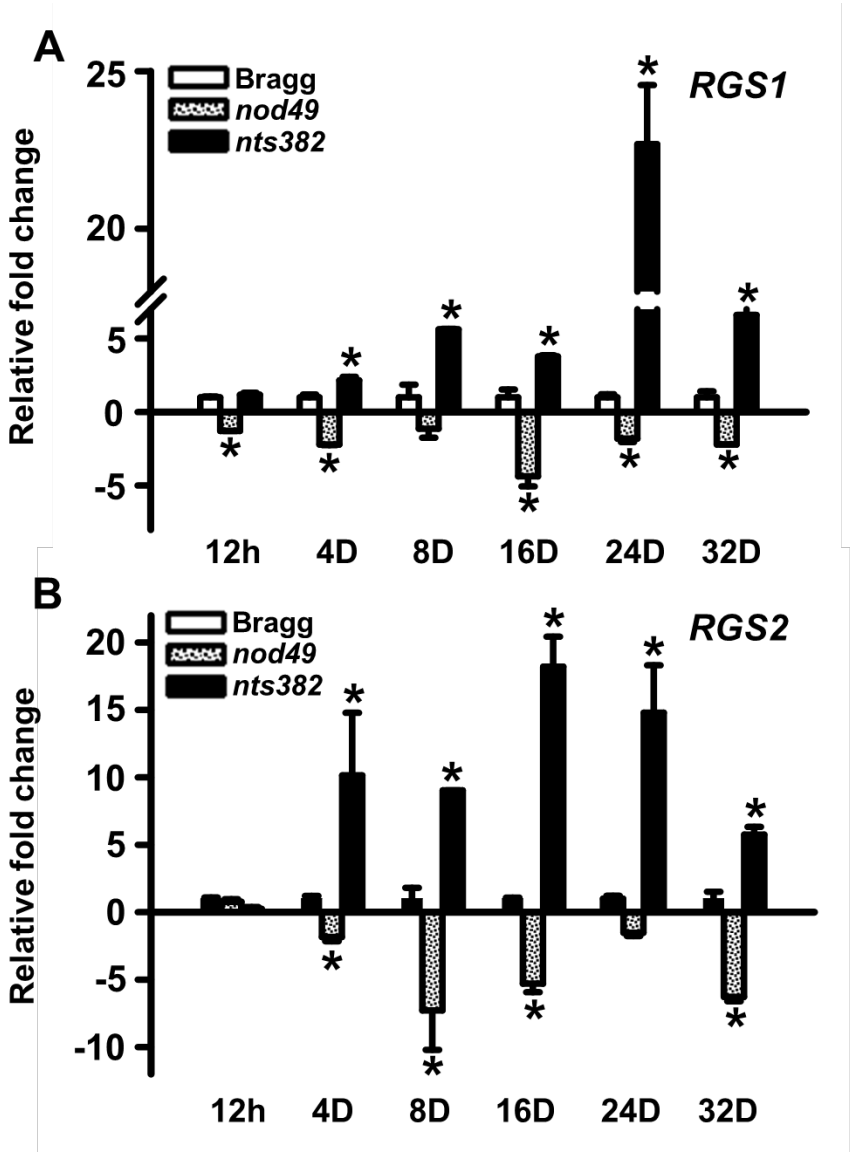

Supplemental Figure 4. *B. japonicum*–induced expression of soybean *RGS1* and *RGS2* in wild type, non-nodulating and super-nodulating soybean hairy roots at different time points. Relative fold changes of (A) *RGS1* and (B) *RGS2* were determined in Bragg (wild-type), *nod49* (non-nodulating) and *nts382* (super-nodulating) soybean hairy roots by real-time PCR after 12 hour (12h), 4 day (4D), 8 day (8D), 16 day (16D), 24 day (24D) and 32 day (32D) post inoculation with *B. japonicum*. Data are normalized by the reference gene *Actin* and 3 biological replicates of three different experiments were used. Error bars represent ± SE. Expression in wild-type Bragg was set at 1. Asterisks (*) represent statistically significant differences compared to empty vector control (* = $P < 0.05$; Student's *t* test).

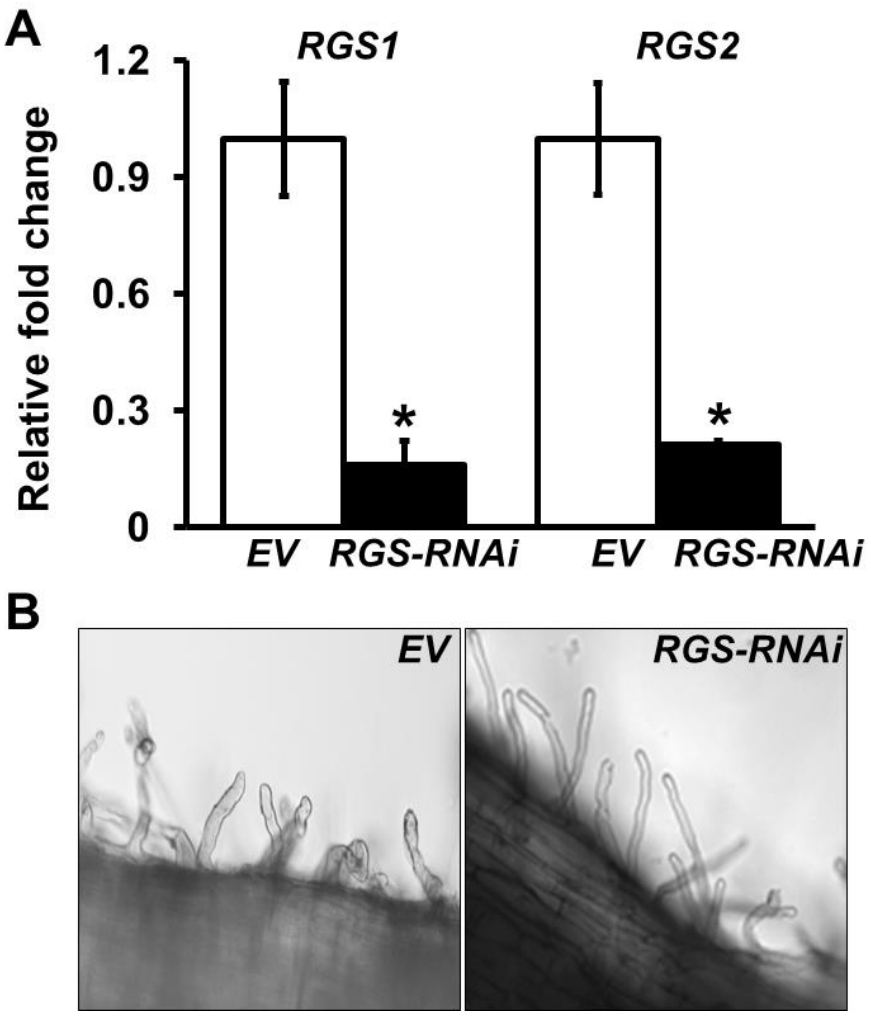

Supplemental Figure 5. Study of expression levels of *RGS* genes and root hair deformation in *RGS-RNAi* silenced transgenic hairy roots. (A) Hairy roots of soybean were collected from *RGS-RNAi* lines 32 dpi with *B. japonicum*. Expression of *RGS1* and *RGS2* in *RGS-RNAi* silenced hairy roots were measured by real-time quantitative PCR. Fold change represents expression of genes in transgenic lines in comparison to their expression in empty vector (EV) containing roots, which was set as 1. Data are representative of three independent experiments and are normalized by the reference gene *Actin*. Data are average from two biological replicates of three different experiments. Error bars represent ± SE. Asterisks (*) indicate statistically significant differences compared to empty vector control (* = $P < 0.05$; Student's *t* test). (B) Microscopic view of *RGS-RNAi* and EV transformed root hairs at 4 days after inoculation with *B. japonicum.* Representative images captured from 10-12 different hairy roots of 3 independent experiments are shown.

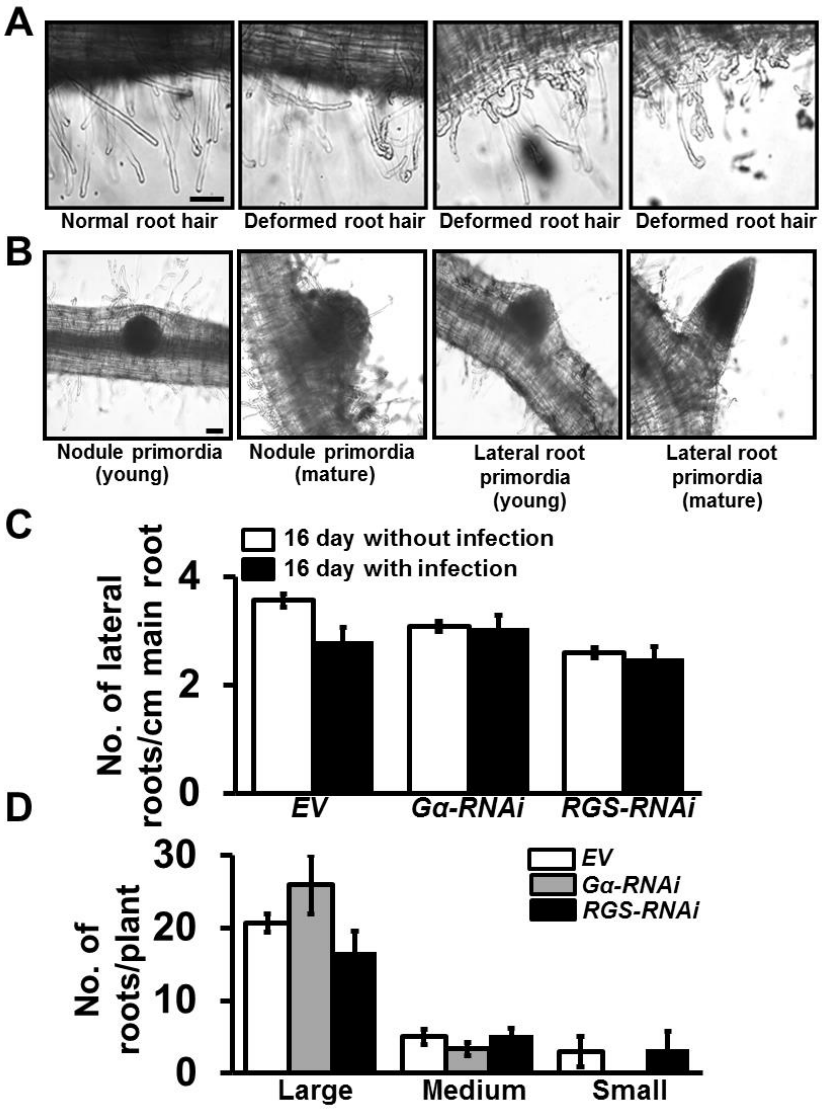

Supplemental Figure 6. Phenotypes of root hairs, lateral root primordia, nodule primordia and roots in *Gα-RNAi* and *RGS-RNAi* transgenic lines. (A) Images of normal and deformed root hairs on soybean hairy roots. Microscopic view of representative root hair deformations observed at 4 days after inoculation with *B. japonicum* is shown. Bar =100 µm. (B) Images of nodule primordia and lateral root primordia on soybean hairy roots. Microscopic view of representative nodule primordia and lateral root primordia developing on transgenic hairy roots is shown. Bar = 500 µm. (C) Quantification of lateral root numbers in soybean *Gα-RNAi* and *RGS*-RNAi transgenic lines. Measurement of lateral root numbers at 16 days after inoculation with *B. japonicum* or without infection. Data are representative of three independent experiments. Error bars represent ± SE. EV (empty vector). (D) Quantification of different sized roots in soybean *Gα-RNAi* and *RGS-RNAi* transgenic lines. Hairy roots were measured and grouped into three different size bins (large > 5 cm, medium = 2.5 cm to 5 cm and small < 2.5 cm) at 32 days after inoculation with *B. japonicum*. Data are representative of three independent experiments. Error bars represent ± SE.

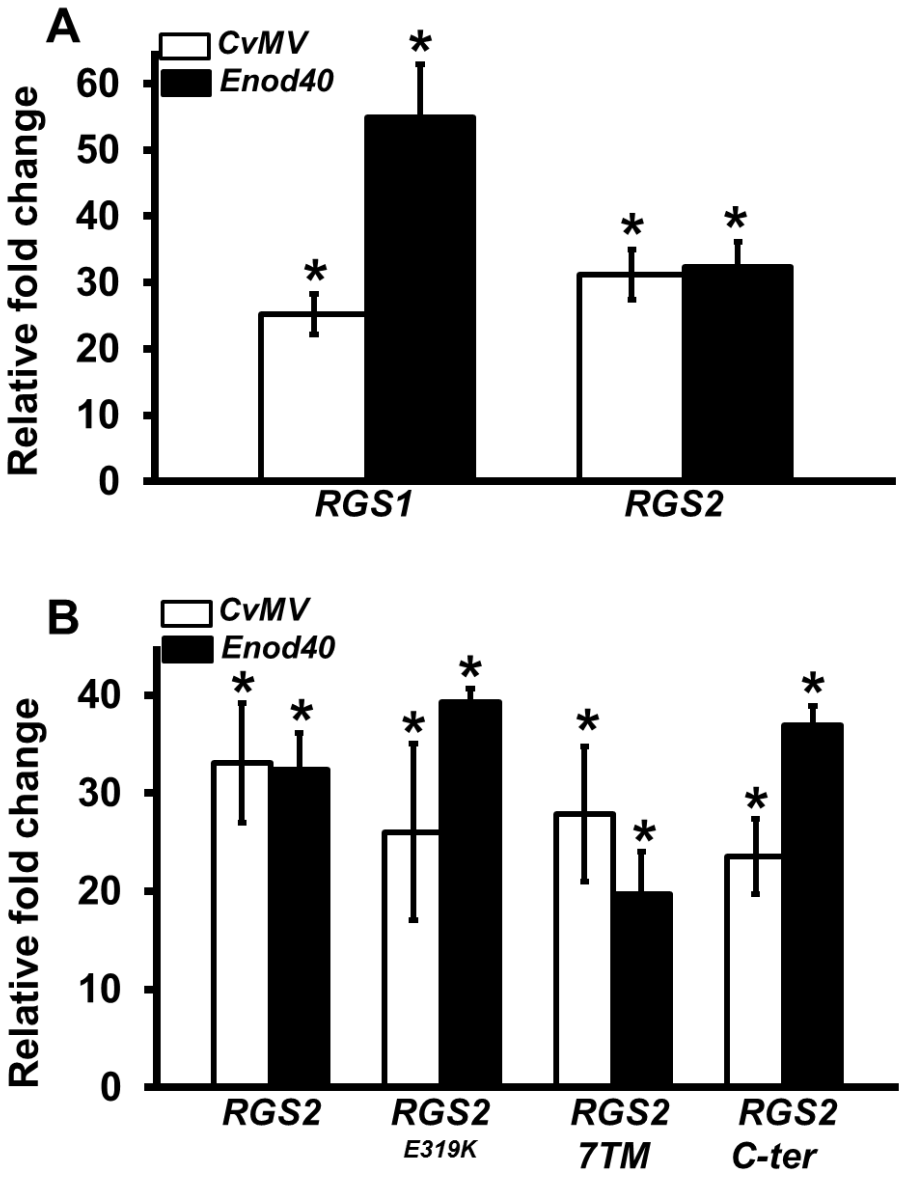

Supplemental Figure 7. Expression levels of *RGS* genes in *RGS*-overexpressing transgenic hairy roots. Hairy roots of soybean were collected from *RGS1* and *RGS2* over-expression lines at 32 dpi with *B. japonicum*. (A) Expression level of *RGS1* and *RGS2* driven by both *CvMV* and *Enod40* promoter. (B) Expression level of native and mutant versions of *RGS2* driven by both *CvMV* and *Enod40* promoter. Fold change was determined by comparing the transcript levels of specific genes in overexpression lines to their expression in EV control lines. Data are representative of three independent experiments and are normalized by the reference gene *Actin*. Error bars represent ± SE. Asterisks (*) indicate statistically significant differences compared to empty vector control (* = $P < 0.05$; Student's *t* test).

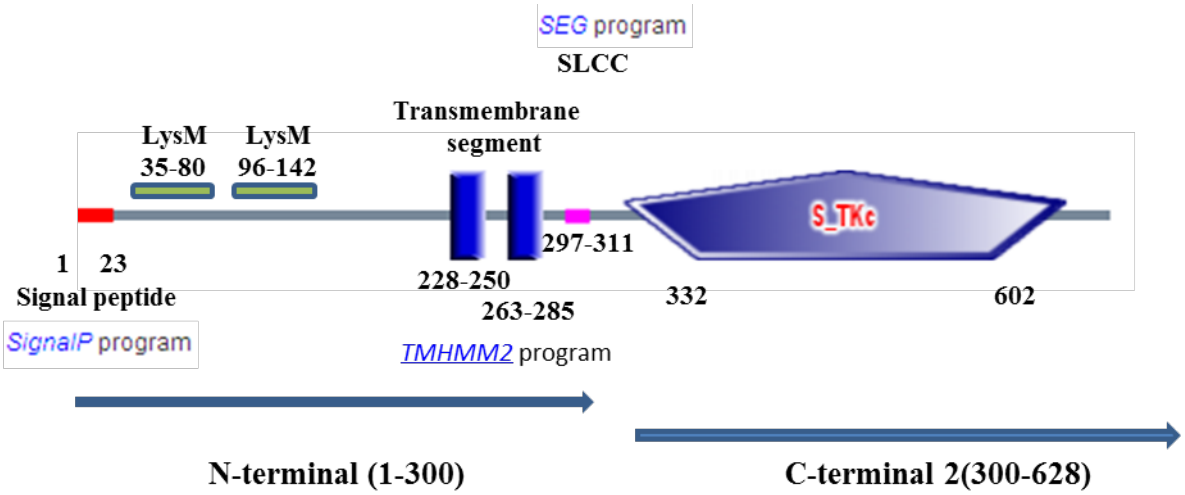

Supplemental Figure 8. Domain architecture of soybean NFR1α. Soybean NFR1α has a signal peptide, two LysM motifs and two transmembrane domain at N-terminal regions and it contains a serine-threonine kinase domain at its C-terminal region.

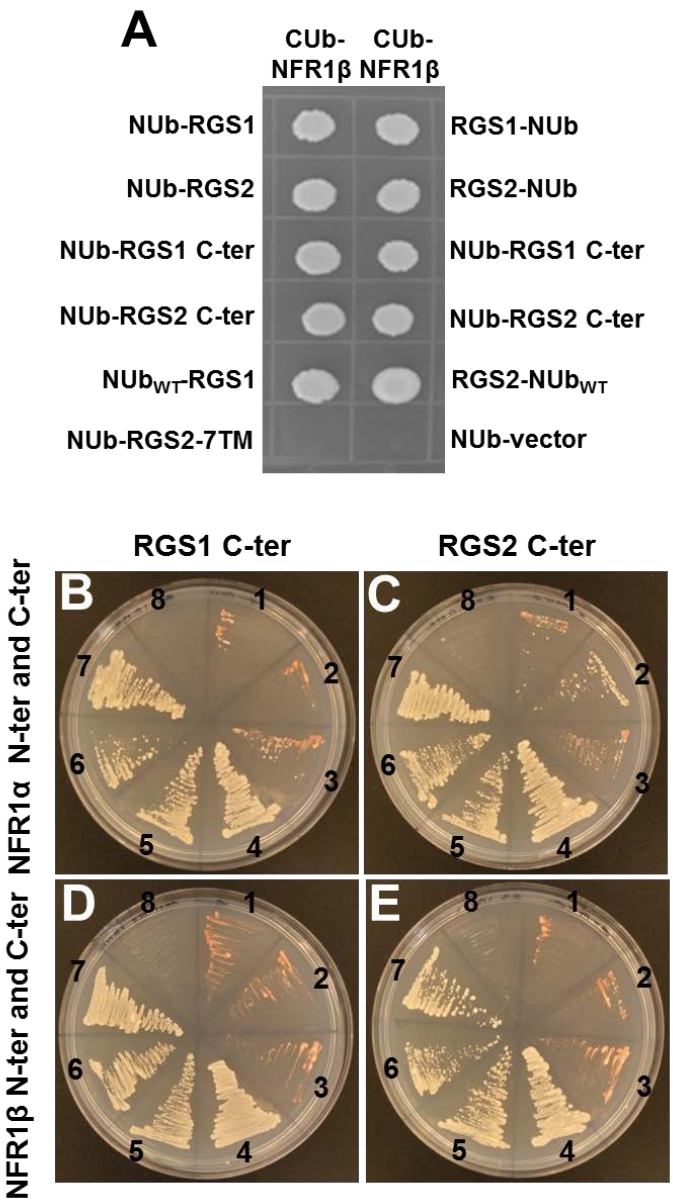

Supplemental Figure 9. Interaction between soybean RGS1 and RGS2 with NFR1α and NFR1β using split ubiquitin-based interaction assay. (A) The picture shows yeast growth on selective media with 200 µM methionine. In all cases, full-length RGS, the N-terminal 7 transmembrane region (7TM) and the C-terminus RGS domain containing RGS were used as NUb fusions in both orientations (NUb-RGS denoting NUb fused to the N terminus of RGS and RGS-NUb denoting NUb fused to the C terminus of RGS). NFR1β was used as CUb fusion. NUbwt fusion and NUb-vector fusion constructs were used as positive and negative controls, respectively. Two biological replicates of the experiment were performed with identical results. (B) and (C), Interaction between NFR1α N- and C-terminal with RGS1 and RGS2 C-terminal; (D) and (E), Interaction between NFR1β N- and C-terminal with RGS1 and RGS2 C-terminal. Two biological replicates of the experiment were performed with identical results. In all cases RGS was used as NUb fusions in both orientations (NUb-RGS; N-terminal of ubiquitin fused at the N-terminal of RGS and RGS-NUb; N-terminal of ubiquitin fused at the C-terminal of RGS) and NFR1 was used as CUb fusion (NFR1α/NFR1β-CUb). NUbwt fusion and NUb-vector fusions constructs were used as positive and negative controls, respectively. The interaction combinations are: (1) NFR1 N-terminal-CUb + RGS-NUb; (2) NFR1 N-terminal-CUb + NUb-RGS; (3) NFR1 N-terminal-CUb + RGS-NUbwt; (4) NFR1 N-terminal-CUb + Nubwt-RGS; (5) NFR1 C-terminal-CUb + RGS-NUb; (6) NFR1 C-terminal-CUb + NUb-RGS; (7) NFR1 C-terminal-CUb + RGS-NUbwt (positive control); (8) NFR1 C-terminal-CUb + NUb-vector (negative control).

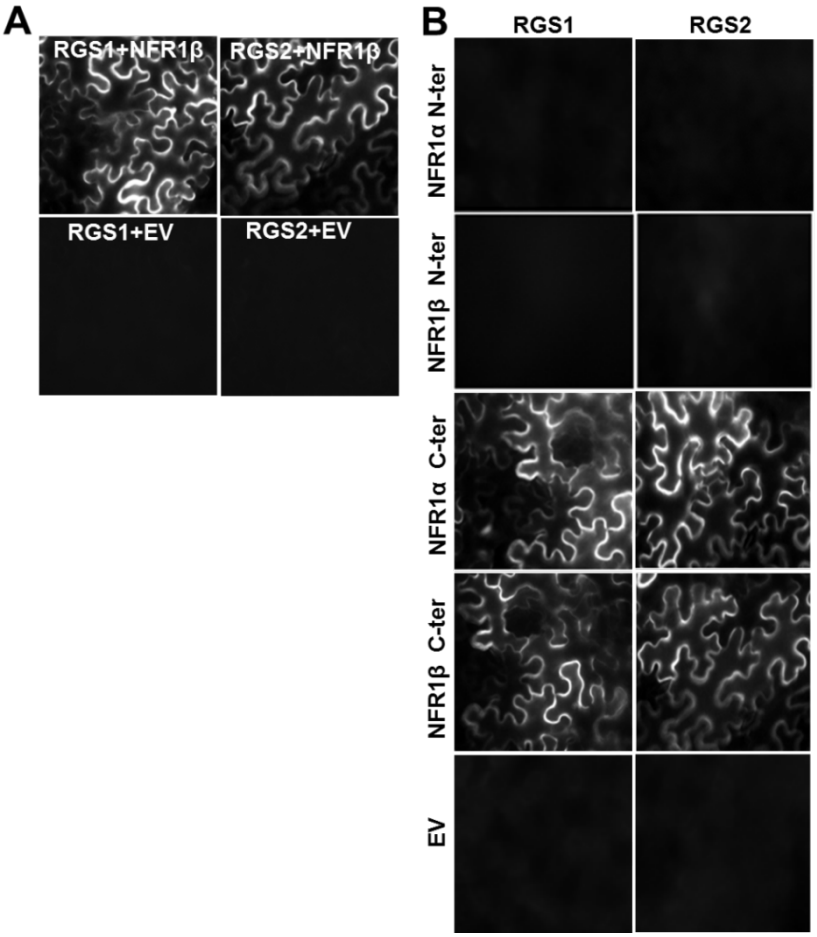

Supplemental Figure 10. Interaction between RGS (in 77-nEYFP-N1) and NFR1 (in 78-cEYFP-N1) using bimolecular fluorescence complementation assay. Agrobacteria containing different combination of soybean RGS1 and RGS2 and NFR1 (α, β) were infiltrated in tobacco leaves and reconstitution of YFP fluorescence due to protein-protein interaction was recorded. Infiltrated plants were incubated in darkness for 24 h followed by 36 h incubation in light. The leaves were observed under Nikon Eclipse E800 microscope with epi-fluorescent modules for YFP fluorescence detection. At least five independent infiltrations were performed for each construct. (A) Interaction between full-length RGS with NFR1β using bimolecular fluorescence complementation assay. (B) Interaction between full-length RGS with N-and C-terminal NFR1 using bimolecular fluorescence complementation assay. The interaction combinations are: RGS1/RGS2+NFR1α N-terminal, RGS1/RGS2+NFR1β N-terminal, RGS1/RGS2+NFR1α C-terminal, RGS1/RGS2+ NFR1β C-terminal, RGS1/RGS2 + EV. Interaction between soybean RGS1 and RGS2 with empty vector were used as negative controls.

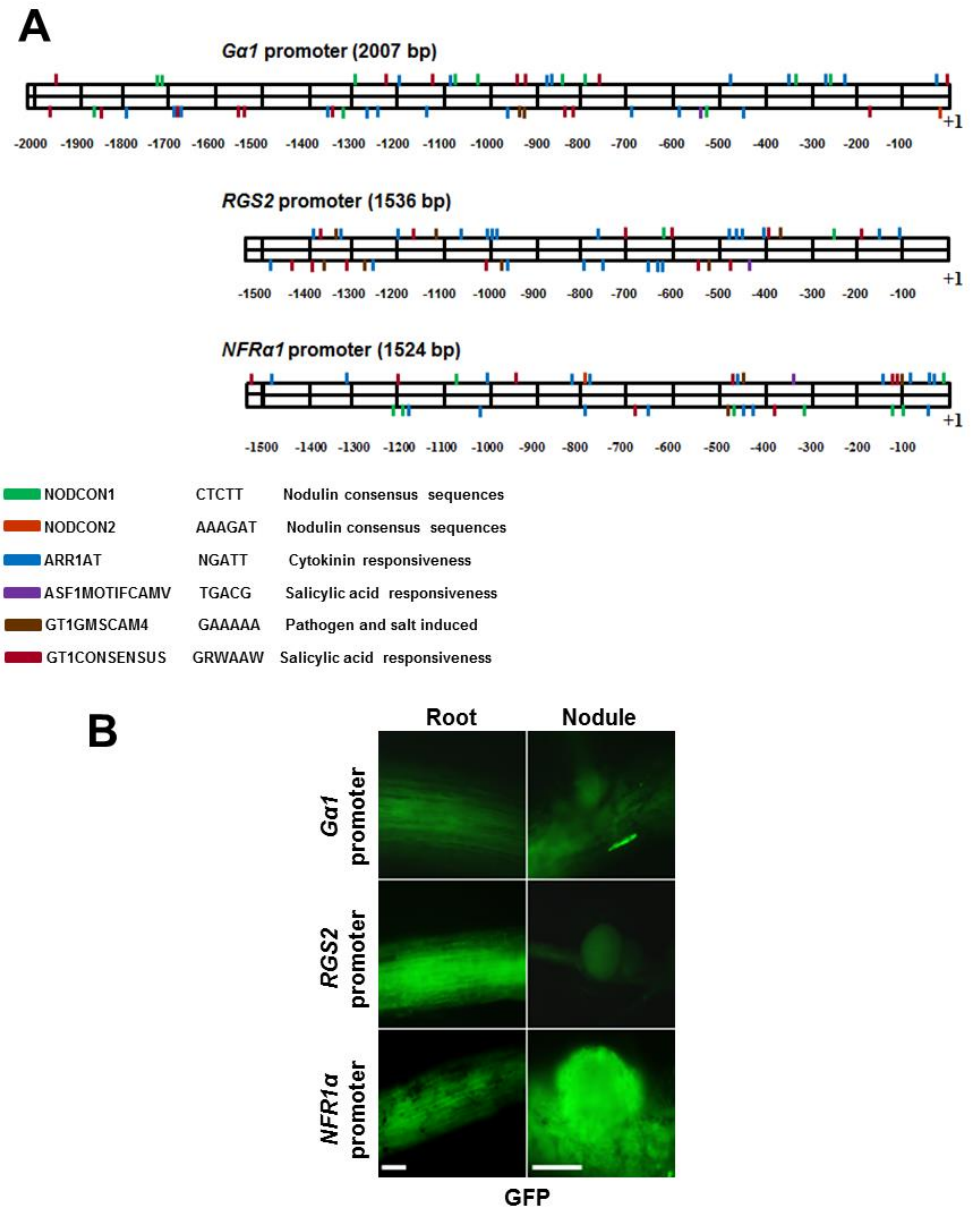

Supplemental Figure 11. Analysis of promoter of *Gα1*, *RGS2* and *NFR1α*. (A) The cis-elements within the promoter of *Gα1* (~2 Kb), *RGS2* (~1.5 Kb) and *NFR1α* (~1.5 Kb) were identifying using PLACE database (K. Higo, Y. Ugawa, M. Iwamoto and T. Korenaga (1999) Plant cis-acting regulatory DNA elements (PLACE) database: 1999. Nucleic Acids Research Vol. 27 No.1 pp. 297-300.). (http://www.dna.affrc.go.jp/PLACE/). **(B)** The constructs containing the pro *Gα1*:*GFP*, pro *RGS2*:*GFP* and pro *NFR1α*:*GFP* were transformed using the hairy root transformation system and detection of GFP fluorescence was observed 10 days after *B. japonicum* infection in hairy roots and 24 days after infection in nodules. Bar = 150 μm and 1 mm for hairy roots and nodules, respectively.

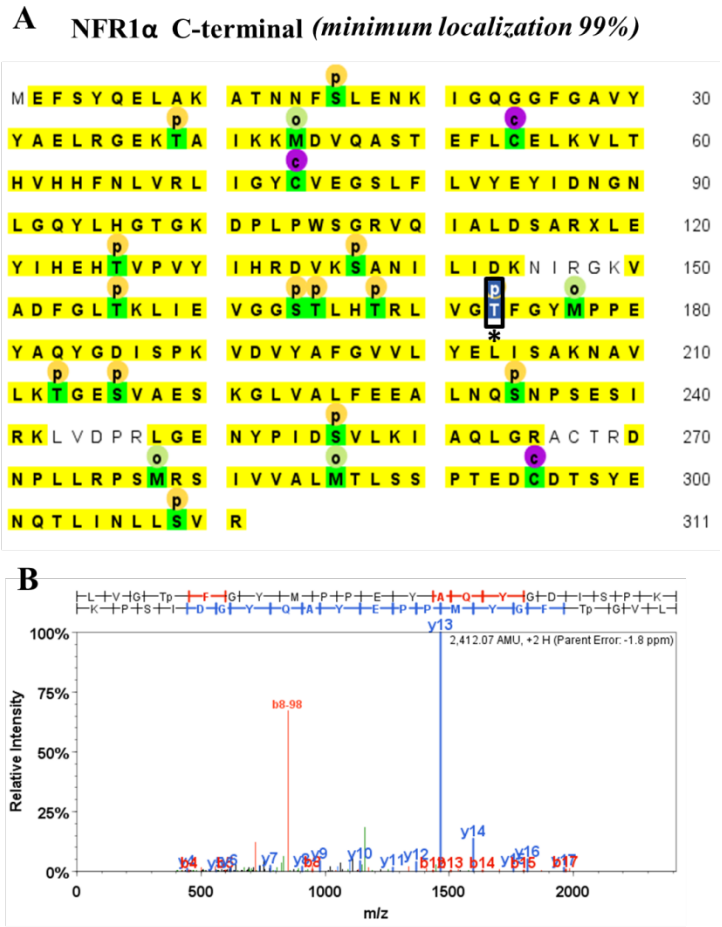

Supplemental Figure 12. Detection of phosphorylated amino acid residues in NFR1α C-terminal kinase domain by LC-MS/MS after *in vitro* phosphorylation assay. (A) Kinase C-terminal protein sequence identified with 95% coverage (highlighted in yellow) using a peptide probability threshold of 80% calculated according to the Peptide Prophet algorithm. Phosphorylation modifications of serine and threonine residues were identified as indicated in the figure p. Other experimental modifications (oxidation of methionine and carbamidomethylation of cysteine) are also shown in the figure although not relevant here. The localization probability of the phosphorylation sites was further tested using Scaffold PTM (v2.1.2.1 Proteome Software). The threshold was set to 95% localization probability. The most important phosphorylation residue within the activation loop is indicated by * sign. (B) The figure shows the fragmentation profile of one specific peptide identified as LVG**Tp**FGYMPPEYAQYGDISPK with a phosphorylation site at threonine 173 (C-terminal region, corresponds to threonine 473 residue in full-length protein) and localization probability of 100. The y and b ions coverage as shown in the figure is evidence that the phosphorylation of the phosphopeptide is located on the threonine.

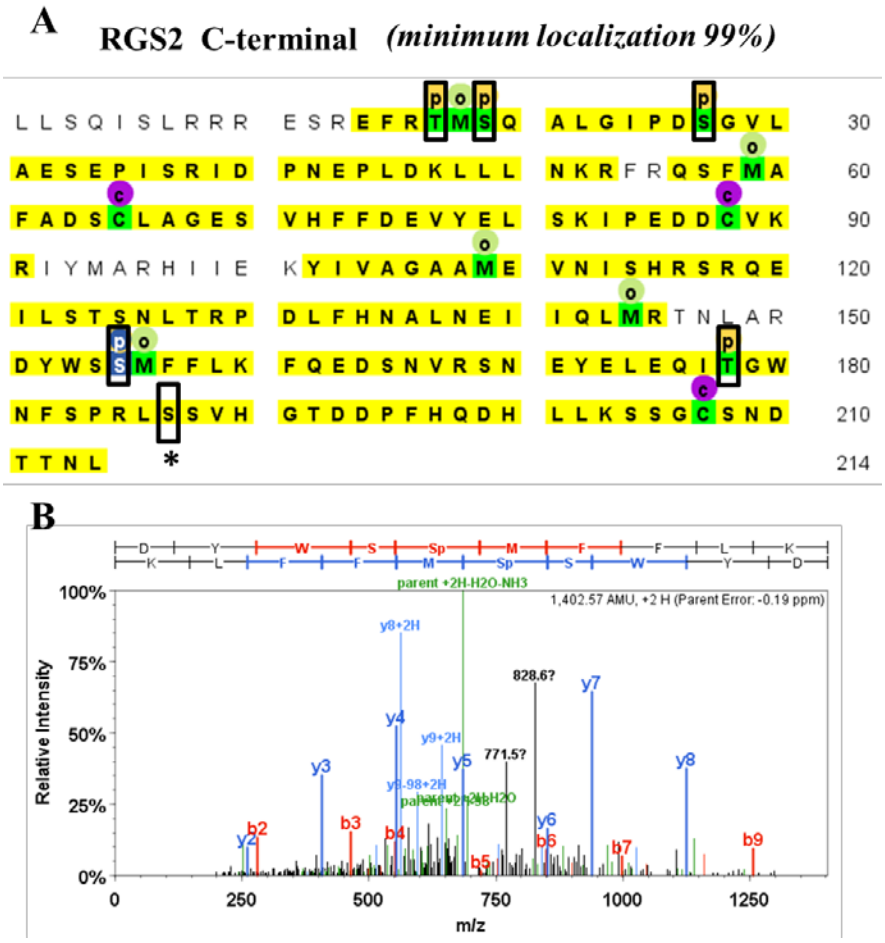

Supplemental Figure 13. Detection of phosphorylated amino acid residues in RGS2 C-terminal region by LC-MS/MS after *in vitro* phosphorylation assay. (A) The figure shows the RGS2 C-terminal protein sequence identified with 95% coverage (highlighted in yellow) using a peptide probability threshold of 80% calculated according to the Peptide Prophet algorithm. Phosphorylation modifications of serine and threonine residues were identified as indicated in the figure p. Other experimental modifications (oxidation of methionine and carbamidomethylation of cysteine) are also shown in the figure although not relevant here. The localization probability of the phosphorylation sites was further tested using Scaffold PTM (v2.1.2.1 Proteome Software). The threshold was set to 95% localization probability. Another important phosphorylation residue is indicated by * sign and this residue were detected when the threshold was set to 80% localization probability. (B) The figure shows the fragmentation profile of one specific peptide identified as DYWS**Sp**MFFLK with a phosphorylation site at serine 155 in C terminal region (corresponds to serine 405 in full-length protein) and localization probability of 100. The y and b ions coverage as shown in the figure is evidence that the phosphorylation of the phosphopeptide is located on the serine.

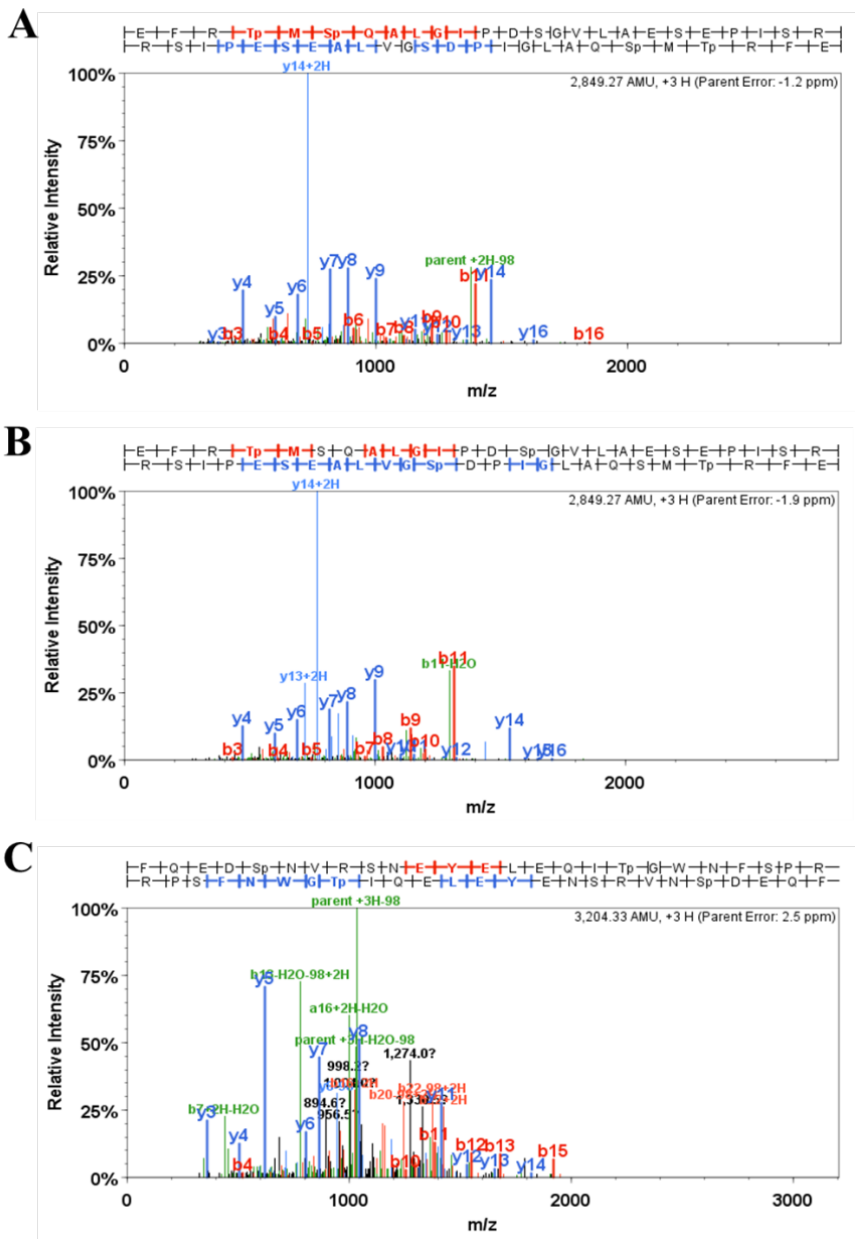

Supplemental Figure 14. Detection of phosphorylation sites within soybean RGS2 C-terminal region by LC-MS/MS after *in vitro* phosphorylation assay. (A) The figure shows the fragmentation profile of one specific peptide identified as EFR**Tp**M**Sp**QALGIPDS GVLAESEPISR with a phosphorylation site at threonine 17 and serine 19 in C terminal region (correspond to threonine 267 and serine 269 residue in full-length protein) and localization probability of 100. (B) The figure shows the fragmentation profile of one specific peptide identified as EFRTpMSQALGIPD**Sp** GVLAESEPISR with a phosphorylation site at serine 27 in C terminal region (corresponds to serine 277 residue in full-length protein) and localization probability of 100. (C) The figure shows the fragmentation profile of one specific peptide identified as FQEDSpNVRSNEYELEQI**Tp**GWNFSPR with a phosphorylation site at threonine 178 in C terminal region (corresponds to threonine 437 in full-length protein) and localization probability of 100. In all cases, the y and b ions coverage as shown in the figures is evidence that the phosphorylation of the phosphopeptide is located on either serine/threonine.

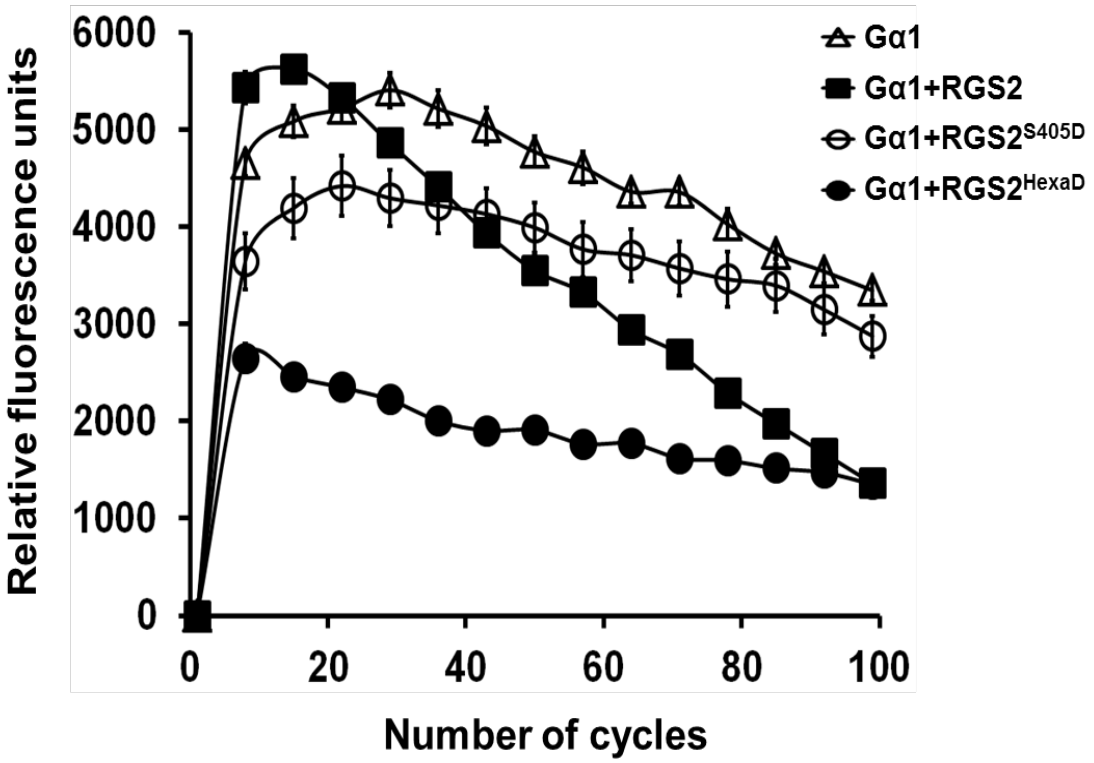

Supplemental Figure 15. Changes of GTPase activity of Gα1 in the presence of different mutant versions of RGS2. GTP hydrolysis was measured using GTP-BODIPY-FL in real time fluorescence assays. GTPase activity of Gα1 was measured in absence or presence of purified recombinant C-terminal native and mutant RGS2. Data are one of two independent experiments, each with three replicates, mean ± S.E.

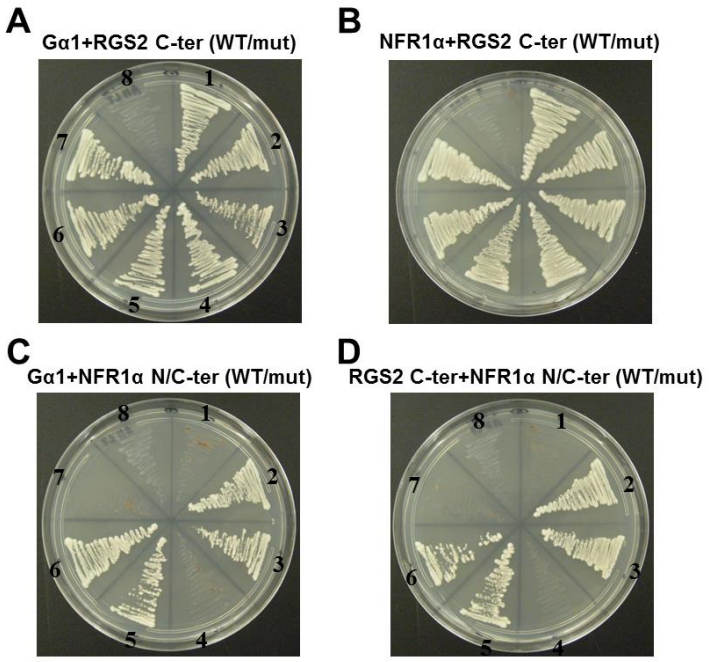

Supplemental Figure 16. Interaction between Gα1 with wild type and mutant RGS2 and NFR1α using split ubiquitin-based interaction assay. (A) C-terminal RGS2 was used as CUb fusion (RGS2-CUb) and Gα1 were used as NUb fusions in both orientations (NUb-Gα; N-terminal of ubiquitin fused at the N terminal of Gα and Gα-NUb; N-terminal of ubiquitin fused at the C-terminal of Gα). NUbwt fusion constructs were used as positive controls for interaction and NUb-vector fusions were used as negative controls. The interaction combinations are: (1) C-terminal RGS2-CUb + Gα1-NUb; (2) C-terminal RGS2^{S405A}-CUb + Gα1-NUb; (3) C-terminal RGS2^{HexaA}-CUb + Gα1-NUb; (4) C-terminal RGS2-CUb + NUb-Gα1; (5) C-terminal RGS2^{S405A}-CUb + NUb-Gα1; (6) C-terminal RGS2^{HexaA}-CUb + NUb-Gα1; (7) C-terminal RGS2-CUb + NUbwt-Gα1 (positive control) and (8) C-terminal RGS2-CUb+NUb-vector (negative control). (B) C-terminal RGS2 was used as CUb fusion (RGS2-CUb) and NFR1α was used as NUb fusion in both orientations. The interaction combinations are: (1) C-terminal RGS2-CUb + NFR1α-NUb; (2) C-terminal RGS2^{S405A}-CUb + NFR1α-NUb; (3) C-terminal RGS2^{HexaA}-CUb + NFR1α-NUb; (4) C-terminal RGS2-CUb + NUb-NFR1α; (5) C-terminal RGS2^{S405A}-CUb + NUb-NFR1α; (6) C-terminal RGS2^{HexaA}-CUb + NUb-NFR1α; (7) C-terminal RGS2-CUb + NUbwt-NFR1α (positive control) and (8) C-terminal RGS2-CUb+NUb-vector (negative control). (C) NFR1α was used as CUb fusion (NFR1α-CUb) and Gα1 was used as NUb fusion in both orientations. The interaction combinations are: (1) NFR1α N-terminal-CUb + Gα1-NUb; (2) NFR1α C-terminal-CUb + Gα1-NUb; (3) NFR1α C-terminal^{T473A}-CUb + Gα1-NUb; (4) NFR1α N-terminal-CUb + NUb-Gα1; (5) NFR1α C-terminal-CUb+NUb-Gα1; (6) NFR1α C-terminal^{T473A}-CUb +NUb-Gα1; (7) NFR1α N-terminal-CUb + NUb-vector (negative control) and (8) NFR1α C-terminal-CUb + NUb-vector (negative control). (D) NFR1α was used as CUb fusion (NFR1α-CUb) and C-terminal RGS2 was used as NUb fusion in both orientations. The interaction combinations are: (1) NFR1α N-terminal-CUb + C-terminal RGS2-NUb; (2) NFR1α C-terminal-CUb + C-terminal RGS2-NUb; (3) NFR1α C-terminal^{T473A}-CUb + C-terminal RGS2-NUb; (4) NFR1α N-terminal-CUb + NUb-C-terminal RGS2; (5) NFR1α C-terminal-CUb + NUb-C-terminal RGS2; (6) NFR1α C-terminal^{T473A}-CUb + NUb- C-terminal RGS2; (7) NFR1α N-terminal-CUb + NUb-vector (negative control) and (8) NFR1α C-terminal-CUb + NUb-vector (negative control). In all cases two biological replicates of the experiment were performed with identical results. The picture shows yeast growth on selective media with 200 µM methionine.

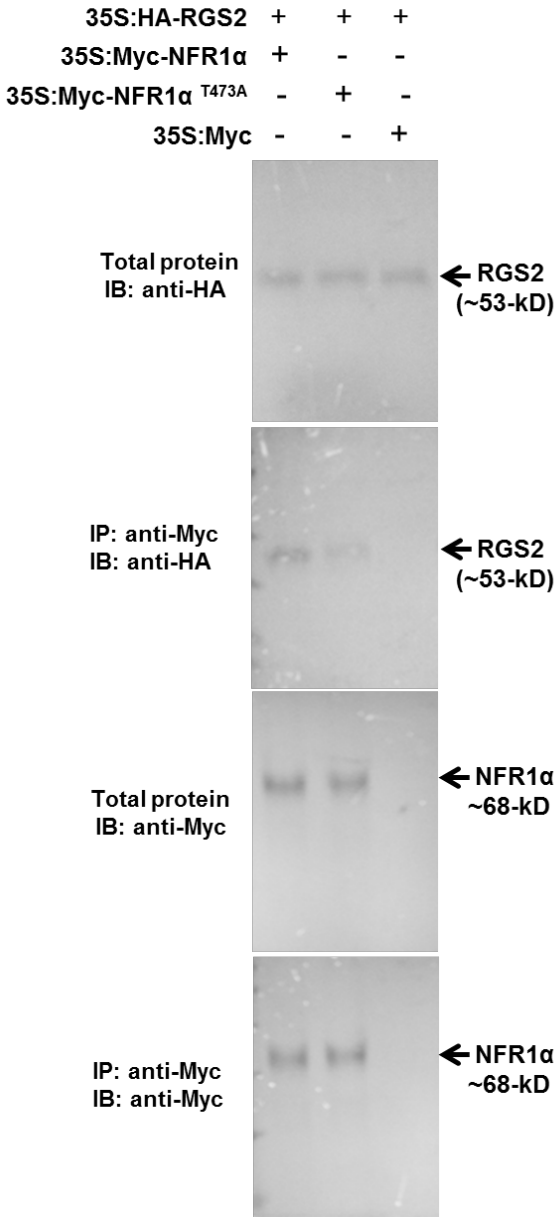

Supplemental Figure 17. Myc-tagged wild type NFR1α and mutant NFR1α^{T473A} associate with soybean RGS2 *in vivo*. Total proteins were extracted from tobacco leaves infiltrated with 35S:HA-RGS2, 35S:Myc-NFR1α, 35S:Myc-NFR1α^{T473A} and 35S:Myc-tagged empty vector in different combinations. Anti-Myc antibody was used for immunoprecipitation, and the total extracts and precipitates were further immunoblotted with HA and Myc antibodies to detect the RGS2 and NFR1α.

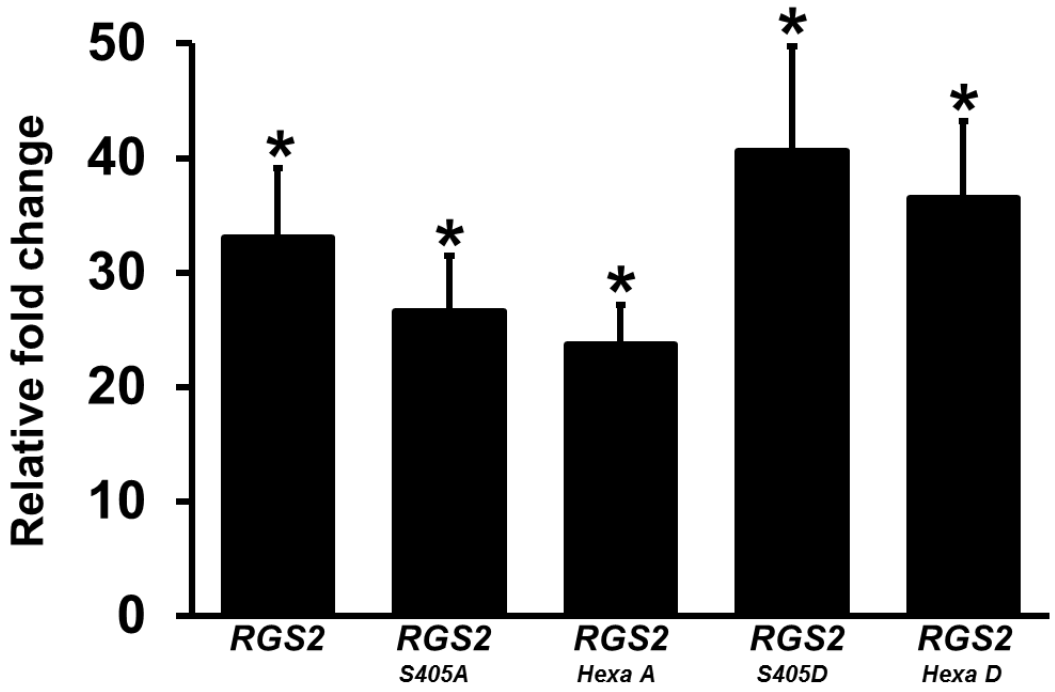

Supplemental Figure 18. Transcript level of soybean *RGS2* in native and mutant *RGS*-overexpressing hairy roots. Hairy roots of soybean were collected from specific *RGS*-overexpression lines 32 days after inoculation with *B. japonicum*. Expression of *RGS2* driven by both *CvMV* and *Enod40* promoter were measured by real-time quantitative PCR. Fold change represents expression of genes in transgenic lines in comparison to their expression in empty vector (EV) containing roots, which was set as 1. Data are representative of three independent experiments and are normalized by the reference gene *Actin*. Error bars represent ± SE. Asterisks (*) indicate statistically significant differences compared to empty vector control (* = $P < 0.05$; Student's *t* test).

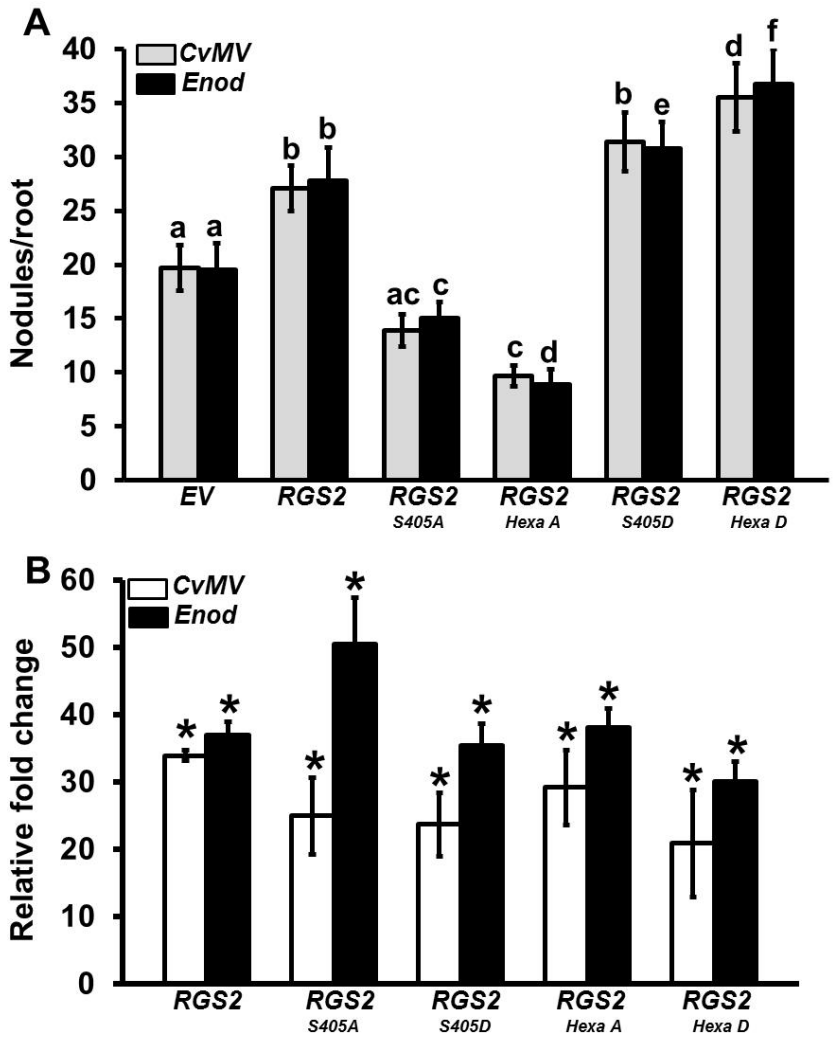

Supplemental Figure 19. Nodule formation on transgenic soybean hairy roots over-expressing phospho-dead and phospho-mimic versions of C-terminal RGS2. (A) Native *RGS2*, single mutant phospho-dead and phospho-mimic versions (*RGS2*^{S405A} and *RGS2S*^{405D}) and hexa mutant phospho-dead and phospho-mimic versions (*RGS2*^{HexaA} and *RGS2*^{HexaD}) of C-terminal *RGS2* driven by *CvMV* and *Enod40* promoter were used for hairy root transformation. Nodule number in over-expression roots was counted at 32 dpi with *B. japonicum* and compared with the empty vector containing hairy roots. The data represent average of 3 biological replicates (40-50 individual plants/biological replicate) containing transgenic nodulated roots. Different letters indicate a significant difference (Dunn's multiple comparisons test, $P < 0.05$) (B) Transcript level of soybean *RGS2* in native and mutant *RGS*-overexpressing hairy roots. Hairy roots of soybean were collected from specific *RGS*-overexpression lines 32 days after inoculation with *B. japonicum*. Expression of *RGS2* driven by both *CvMV* and *Enod40* promoter were measured by real-time quantitative PCR. Fold change represents expression of genes in transgenic lines in comparison to their expression in empty vector (EV) containing roots, which was set as 1. Data are representative of three independent experiments and are normalized by the reference gene *Actin*. Error bars represent ± SE. Asterisks (*) indicate statistically significant differences compared to empty vector control (* = $P < 0.05$; Students *t* test).

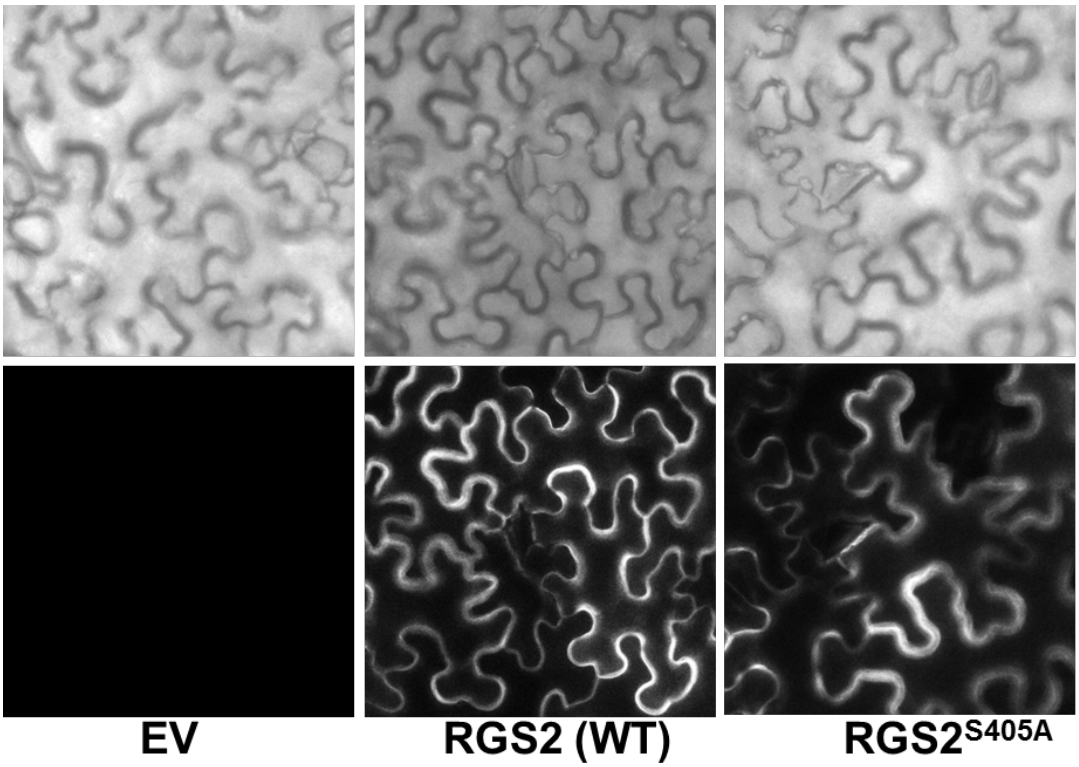

Supplemental Figure 20. Localization of native and mutant RGS2. Native *YFP-RGS2* and *YFP-RGS2*^{S405A} mutant protein both localize to the cell periphery in transiently transformed tobacco leaves. At least six independent transformations were performed. The figure shows representative picture from one transformation. Empty vector was used as negative control. Upper panel: bright field images of the represented leaves.

Supplemental Data. Roy Choudhury and Pandey (2015). Plant Cell 10.1105/tpc.15.00517

Supplemental Table 1. Primers used in experiments described in the manuscript.

Gene expression:	
Gα1 RT FP	CTCCAAGTTCCAGATTGTGCC
Gα1 RT RP	TCAAAACATGGTTGCCTTAGGAC
Gα2 RT FP	TTCAGGAGACATATGCCCGA
Gα2 RT RP	GGATCCACTCGAAAAGTTCCTTG
Gα3 RT FP	AATTTGCAAAGGCTGTCTGACA
Gα3 RT RP	ACTCGAAAAGTTCCTTAGTCTCGG
Gα4 RT FP	AGCTTGCACAGGAAATAGAGAGA
Gα4 RT RP	CCATTTTCTCCTCTCATTTCTCTGA
RGS1 RT FP	ATACCTGAAGATGACTGTGTGAG
RGS1 RT RP	TGAAGACCAGTAATCTCGAGCT
RGS2 RT FP	TAAAATACCTGAAGATGACTGTGTTAA
RGS2 RT RP	GAAGACCAGTAATCTCGGGCC
NFR1α RT FP	GGT GCG CTT GAT TGG ATA TT
NFR1α RT RP	ATT CAA GGC CTC TTG CTG AA
ENOD40 RT FP	GAA AGG GGT GTG AGA GGA GAG
ENOD40 RT RP	CGC CAC TCA AGA AAG AAT GTT
NODULIN 35 RT FP	CAC TTC CTG ATA CCC GTG AAA
NODULIN 35 RT RP	AAA GTA AAG CGG CTT CTG AGG
Apyrase GS52 RT FP	AAG ATC TTC CCC AAA CAG GAA
Apyrase GS52 RT RP	CAA GTT CTG GTC GAA ATG GAA
Calmodulin-like protein RT FP	TCTCCCAGTCCAAGATCACC
Calmodulin-like protein RT FP	GCCGATATTTTCCCATCTCC
Split ubiquitin based Yeast two hybrid:	
Gα SUS FP	ACAAGTTTGTACAAAAAAGCAGGCTCTCCAACCACCA TGGGCTTASTCTGYAGCAG
Gα SUS RP	TCCGCCACCACCAACCACTTTGTACAAGAAAGCTGG GTATAAYAAGCCAGCYTC
RGS SUS FP	ACAAGTTTGTACAAAAAAGCAGGCTCTCCAACCACCA TGGTGACCTGTGCCGTGAA
RGS SUS RP	TCCGCCACCACCAACCACTTTGTACAAGAAAGCTGG GTATAAATYAGTTGTATCATTGCT
RGS 7TM SUS RP	TCC GCC ACC ACC AAC CAC TTT GTA CAA GAA AGC TGG GTA TGG TTG TGA ACT TGA TAT TG
RGS C-terminal SUS FP	ACA AGT TTG TAC AAA AAA GCA GGC TCT CCA ACC ACC CTT CTC TCA CAA ATC AGC TTG AGG
NFR1α SUS FP	TCC GCC ACC ACC AAC CAC TTT GTA CAA GAA AGC TGG GTA GGA TCC TGA AGT TTC ATA TTC
NFR1α/β N-terminal SUS RP	ACA AGT TTG TAC AAA AAA GCA GGC TCT CCA ACC ACC TGG TAT TAT CAG CAT ATT GAG

NFR1 α/β SUS RP	ACA AGT TTG TAC AAA AAA GCA GGC TCT CCA ACC ACC AGT GGG ACT GCT AGT GCT ACT
NFR1β SUS FP	ACA AGT TTGTACAAAAAAGCAGGCTCTCCAACCACC ATGGAACTCAAAAAATGGTTACTG
BiFC	
NFR1α BiFc FP	CAGATCCTCGAGCATGGAACTCAAAAAAGGG
NFR1α/β BiFc RP	CAGATCGAATTCTCTCACAGACAGTAGATT
NFR1β BiFc FP	CAGATCCTCGAGCATGGAACTCAAAAAATGG
NFR1α BiFc C-terminal FP	CAGATCCTCGAGCAGTGGGACTGCTAGTGCTACT
NFR1 β BiFc C-terminal FP	CAGATCCTCGAGCATGGCGTTTTCAACTCAAGAT
RGS1/2 BiFC FP	TCTGCAGTCGACATGGTGACCTGTGCCGTG
RGS1/2 BiFC RP	GGTGGATCCCGGGCCTAAATYAGTTGTATCATT
Cloning and protein expression	
NFR1α FP	ATGGAACTCAAAAAAGGGTTACTTG
NFR1α/β RP	ACATCTCACAGACAGTAGATTTATG
NFR1β FP	ATGGAACTCAAAAAATGGTTACTGT
NFR1α NheI FP	ATGCGCTAGCATGGAACTCAAAAAAGGG
NFR1α/β EcoRI RP	ATGCGAATTCTCATCTCACAGACAGTAG
NFR1α NheI C-terminal FP	ATGCGCTAGCAGTGGGACTGCTAGTGCT
NFR1β NheI C-terminal FP	ATGCGCTAGCATTATGGTGGCAAAATCA
RGS2 FP	ATG GTG ACC TGT GCC GTG AAA GGA G
RGS2 7TM RP	TGG TTG TGA ACT TGA TAT TG
RGS2 RP	TAA ATY AGT TGT ATC ATT GCT
RGS2 RNAi RP	TAACCCACACAGCAATGGACACA
RGS1/2 NheI C-terminal FP	ATTAGCTAGCCTTCTCTCACAAATCAGCTTGA
RGS1/2 NotI C-terminal FP	AATTAAGAATTCTCATAAATYAGTTGTATCATTG
Gα RNAi 1 FP	GAA ATT GGA GGC AGG CTG
Gα RNAi 1 RP	TAT GTC AAA CTT GTT TAA
Gα RNAi 2 FP	GAT GTT GGC GGC CAG AGA
Gα1 NheI FP	ATTAGCTAGCATGGGCTTAGTCTGCAGCAGA
Gα1 EcoRI RP	ATTAGAATTCTCATAATAAGCCAGCTTCAAG
Site directed mutagenesis	
NFR1α T473A FP	CACACTCGTCTTGTGGGAGCATTTGGATACATGCCAC CA
NFR1α T473A RP	TGGTGGCATGTATCCAAATGCTCCCACAAGACGAGT GTG
NFR1α T473D FP	CACACTCGTCTTGTGGGAGATTTTGGATACATGCCAC CA
NFR1α T473D RP	TGGTGGCATGTATCCAAAATCTCCCACAAGACGAGTG TG
RGS2 E319K FP	GAT AGT TGC TTG GCT GGG AAG AGT GTG CAC TTC TTT GAT

RGS2 E319K RP	ATC AAA GAA GTG CAC ACT CTT CCC AGC CAA GCA ACT ATC
RGS2 T267A FP	GAA TCC AGA GAA TTT CGC GCA ATG AGT CAG GCT CTG GGC
RGS2 T267A RP	GCC CAG AGC CTG ACT CAT TGC GCG AAA TTC TCT GGA TTC
RGS2 S269A FP	AGA GAA TTT CGC ACA ATG GCT CAG GCT CTG GGC ATA CCT
RGS2 S269A RP	AGG TAT GCC CAG AGC CTG AGC CAT TGT GCG AAA TTC TCT
RGS2 S277A FP	GCT CTG GGC ATA CCT GAT GCT GGG GTA CTA GCA GAA AGT
RGS2 S277A RP	ACT TTC TGC TAG TAC CCC AGC ATC AGG TAT GCC CAG AGC
RGS2 S405A FP	GCC CGA GAT TAC TGG TCT GCG ATG TTC TTC CTG AAG TTC
RGS2 S405A RP	GAA CTT CAG GAA GAA CAT CGC AGA CCA GTA ATC TCG GGC
RGS2 T428A FP	TAC GAG CTG GAG CAA ATA GCA GGG TGG AAC TTT TCT CCA
RGS2 T428A RP	TGG AGA AAA GTT CCA CCC TGC TAT TTG CTC CAG CTC GTA
RGS2 S437A FP	AAC TTT TCT CCA AGG TTG GCT TCT GTG CAT GGT ACA GAC
RGS2 S437A RP	GTC TGT ACC ATG CAC AGA AGC CAA CCT TGG AGA AAA GTT
RGS2 T267D FP	AGA GAA TCC AGA GAA TTT CGC GAT ATG GAT CAG GCT CTG GGC ATA
RGS2 T267D RP	TAT GCC CAG AGC CTG ATC CAT ATC GCG AAA TTC TCT GGA TTC TCT
RGS2 S269D FP	TCC AGA GAA TTT CGC ACA ATG GAT CAG GCT CTG GGC ATA CCT GAT
RGS2 S269D RP	ATC AGG TAT GCC CAG AGC CTG ATC CAT TGT GCG AAA TTC TCT GGA
RGS2 S277D FP	CAG GCT CTG GGC ATA CCT GAT GAT GGG GTA CTA GCA GAA AGT GAA
RGS2 S277D RP	TTC ACT TTC TGC TAG TAC CCC ATC ATC AGG TAT GCC CAG AGC CTG
RGS2 S405D FP	GCC CGA GAT TAC TGG TCT GAT ATG TTC TTC CTG AAG TTC
RGS2 S405D RP	GAA CTT CAG GAA GAA CAT ATC AGA CCA GTA ATC TCG GGC
RGS2 T428D FP	GAG TAC GAG CTG GAG CAA ATA GAT GGG TGG AAC TTT TCT CCA AGG
RGS2 T428D RP	CCT TGG AGA AAA GTT CCA CCC ATC TAT TTG CTC

	CAG CTC GTA CTC
RGS2 S437A FP	TGG AAC TTT TCT CCA AGG TTG GAT TCT GTG CAT GGT ACA GAC GAT
RGS2 S437A RP	ATC GTC TGT ACC ATG CAC AGA ATC CAA CCT TGG AGA AAA GTT CCA
Gα1 Q223L FP	CTC TTT GAT GTT GGT GGC CTG AGA AAT GAG AGA AGA AAA
Gα1 Q223L RP	TTT TCT TCT CTC ATT TCT CAG GCC ACC AAC ATC AAA GAG
Gα1 G196S FP	GCA AGA GTT CGT ACA ACT AGT GTT GTT GAG ATC CAG TTC
Gα1 G196S RP	GAA CTG GAT CTC AAC AAC ACT AGT TGT ACG AAC TCT TGC